

Spinflation with Angular Potentials

Ruth Gregory* and Dariush Kaviani†

*Institute for Particle Physics Phenomenology and Centre for Particle Theory,
Durham University, South Road, Durham, DH1 3LE, UK*

ABSTRACT: We investigate in detail the cosmological consequences of realistic angular dependent potentials in the brane inflation scenario. Embedding a warped throat into a compact Calabi-Yau space with all moduli stabilized breaks the no-scale structure and induces angular dependence in the potential of the probe D3-brane. We solve the equations of motion from the DBI action in the warped deformed conifold including linearized perturbations around the imaginary self-dual solution. Our numerical solutions show that angular dependence is a next to leading order correction to the dominant radial motion of the brane, however, just as angular motion typically increases the amount of inflation (spinflation), having additional angular dependence also increases the amount of inflation. We also derive an analytic approximation for the number of e-foldings along the DBI trajectory in terms of the compactification parameters.

KEYWORDS: String theory and cosmology; inflation.

*Email: r.a.w.gregory@durham.ac.uk

†Email: dariush.kaviani@durham.ac.uk

Contents

1. Introduction	1
2. The supergravity background	3
3. Brane inflation with an angular potential	7
4. Inflationary analysis	9
5. Summary and conclusions	13

1. Introduction

It is now generally accepted that the very early Universe underwent a period of rapid expansion, known as inflation, resulting in a very nearly flat, homogeneous and isotropic initial state. While a simple scalar field model of inflation with a suitable potential satisfies many of the cosmological requirements, such models are rather ad hoc from the high energy particle theory point of view. The challenge is to find a theory which has a clear derivation from a fundamental high energy theory incorporating gravity at the quantum level. String theory naturally is the prime candidate for such a fundamental theory, but one of the major challenges has been to show that in a non-vanishing fraction of the vast number of string vacua the inclusion of various compactification effects in the effective field theory leaves a suitable inflationary model.

In recent years there has been significant progress within the ‘KKLT’ framework, [1], in which the older idea of brane inflation [2], is realised via the motion of a brane in internal, hidden, extra dimensions [3] (see also [4, 5, 6, 7] and the reviews [8]). In these scenarios the inflaton potential (of the position of a probe D3-brane) is flattened by fine-tuned cancellation of correction terms from moduli stabilizing wrapped branes and bulk effects so that inflation can occur. However, whether or not the potential can be made flat to meet the slow-roll conditions, DBI inflation, [9], is also possible, even when the potential is steep. In this case, while the motion of the brane can be strongly relativistic (in the sense of a large γ -factor) strong warping of the local throat region renders their contribution to the local energy density subdominant to that of the inflaton potential terms.

In either case, the approach taken is to consider a D3-brane moving in a warped throat region of a Calabi-Yau flux compactification of type IIB theory with ISD conditions [10]. However, when the UV end of the warped throat is attached to the compact Calabi-Yau space with all moduli stabilized, violations of ISD conditions with important implications for the action of the brane are expected. In particular, the potential of a mobile D3-brane in the compactified throat geometry receives angular dependent corrections, [5], which until recently, have been largely neglected (although see [6, 11]). In slow roll inflation, it was presumed that the angular directions would stabilise rapidly, with the radial (slow-roll) direction dominating the inflationary trajectory. However, for generic brane motion the effect of angular motion is less clear, particularly in the presence of angular terms in the potential.

Angular motion of branes was initially explored in the probe limit, i.e. where the brane does not back-react at all on either the internal or external dimensions. Unsurprisingly, the angular motion has a conserved momentum, which can give interesting brane universes (see e.g. [12, 13, 14]), however the cosmology of these universes via a mirage, [15], interpretation leads to a rather unsatisfactory picture. Based on the probe understanding, it was conjectured that angular motion would not affect a more realistic inflationary scenario to any great extent, an expectation largely borne out by the “spinflation” study, [16], which found a marginal increase of a couple of e-foldings due to angular motion, coming mainly from the initial stages of inflation before the angular momentum becomes redshifted away. This increase is however parameter sensitive, a point not noted in this original study. In [16], a general DBI-inflationary universe was considered near the tip of the warped deformed conifold throat, the Klebanov-Strassler (KS) solution [17], with a simple radial brane potential; with a more realistic potential including angular terms, the spinflationary picture could potentially be rather different.

In this paper therefore, we investigate the cosmological implications of including angular dependence in the DBI brane inflation scenario. Building on the results of Baumann *et al.* [5], we consider D3-brane motion in the warped throat region of the compact Calabi-Yau subject to UV deformations of the geometry that induce angular dependent corrections in the potential of the probe D3-brane. Taking into account linearized perturbations around the ISD solution, we solve the D3-brane equations of motion from the DBI action with angular dependence induced by the leading correction to the potential allowed by the symmetries of the compactification. Our numerical solutions show that angular dependence tends to increase the inflationary capacity of a trajectory, increasing the number of e-foldings, albeit marginally. To a large extent, the trajectories are still predominantly radial, however, do exhibit rotational motion due to the angular potential.

An important question is how generic such trajectories are. In general, as the brane arrives in the throat, one expects a range of initial conditions in terms of angular values and velocities. We find that the D brane trajectories and number of

e-foldings are dependent more on model parameters than on the initial condition of the brane motion, thus indicating that the results of our investigation are reasonably robust.

2. The supergravity background

In brane inflation, a mobile D3 brane (or anti-brane) is embedded in the internal manifold, with its four infinite dimensions parallel to the 4D noncompact universe. The position of the brane on the internal manifold then provides an effective 4D scalar field - the inflaton. The 10D set-up is assumed to be a flux compactification of type IIB string theory on an orientifold of a Calabi-Yau threefold (or an F-theory compactification on a Calabi-Yau fourfold) [10]. We are interested in the situation where fluxes have generated a warped throat in the internal space, and will be examining primarily the deep throat region.

We are therefore considering backgrounds in low-energy IIB supergravity, which in the Einstein frame can be represented by the action

$$S_{\text{IIB}} = -\frac{1}{2\kappa_{10}^2} \int d^{10}x \sqrt{|g|} \left[\mathcal{R} - \frac{|\partial\tau|^2}{2(\text{Im}\tau)^2} - \frac{|G_3|^2}{12 \text{Im}\tau} - \frac{|\tilde{F}_5|^2}{4 \cdot 5!} \right] + \frac{1}{8i\kappa_{10}^2} \int \frac{C_4 \wedge G_3 \wedge \bar{G}_3}{\text{Im}(\tau)} + S_{\text{loc}}, \quad (2.1)$$

where $\tau = C_0 + ie^{-\phi}$ is the axion-dilaton field, $G_3 = F_3 - \tau H_3$ is a combination of the RR and NSNS three-form fluxes $F_3 = dC_2$ and $H_3 = dB_2$, and

$$\tilde{F}_5 = dC_4 - \frac{1}{2}C_2 \wedge H_3 + \frac{1}{2}B_2 \wedge F_3 \quad (+ \text{dual}) \quad (2.2)$$

is the 5-form field, whose self duality must be imposed by hand. The constant κ_{10}^2 is the 10D gravitational coupling:

$$\kappa_{10}^2 = M_{10}^{-2} = \frac{(2\pi)^7 g_s^2 \alpha'^4}{2}. \quad (2.3)$$

In a flux compactification, we are assuming a block diagonal Ansatz for the metric:

$$ds_{10}^2 = e^{2A(y)} g_{\mu\nu} dx^\mu dx^\nu - e^{-2A(y)} \tilde{g}_{mn} dy^m dy^n, \quad (2.4)$$

in which the warp factor, $e^{4A(y)}$, depends only on the internal coordinates y^m , the internal metric \tilde{g}_{mn} is independent of the spacetime coordinates (and will be taken to be a known supergravity solution) and the 4D metric, $g_{\mu\nu}$, is taken as Minkowski for the computation of the supergravity flux background, but ultimately will be assumed to have an FRW form once the general cosmological solution is sought.

Following [10], we take the self-dual 5-form to be given by

$$\tilde{F}_5 = (1 + \star_{10}) \left[d\alpha(y) \wedge dx^0 \wedge dx^1 \wedge dx^2 \wedge dx^3 \right], \quad (2.5)$$

in the Poincaré invariant case, where $\alpha(y)$ is a function of the internal coordinates. The Einstein equations and 5-form Bianchi identity then imply

$$\tilde{\Delta}\Phi_{\pm} = \frac{e^{8A+\phi}}{24}|G_{\pm}|^2 + e^{-4A}|\nabla\Phi_{\pm}| + \text{local}, \quad (2.6)$$

where $\tilde{\Delta}$ is the Laplacian with respect to the 6D metric \tilde{g}_{mn} , and

$$G_{\pm} \equiv (i \pm \star_6)G_3, \quad \Phi_{\pm} \equiv e^{4A} \pm \alpha. \quad (2.7)$$

For $G_- = 0$, i.e. $\star_6 G_3 = iG_3$, the flux G_3 is imaginary self-dual (ISD), and the background metric \tilde{g}_{mn} is a Calabi-Yau metric with the 5-form flux given by $\alpha = e^{4A}$ [10].

The particular concrete example we will be interested in is where the background is the warped deformed conifold, or Klebanov-Strassler (KS), solution [17]. Here, the internal metric is a strongly warped and deformed throat, which interpolates between a regular $\mathbb{R}^3 \times S^3$ tip, to an $\mathbb{R} \times T^{1,1}$ cone in the UV. The metric is usually presented as:

$$\tilde{g}_{mn}dy^m dy^n = \frac{\epsilon^{4/3}}{2}K(\eta) \left[\frac{1}{3K(\eta)^3} \{d\eta^2 + (g^5)^2\} + \cosh^2 \frac{\eta}{2} \{(g^3)^2 + (g^4)^2\} + \sinh^2 \frac{\eta}{2} \{(g^1)^2 + (g^2)^2\} \right], \quad (2.8)$$

in which η is a coordinate chosen so that the function K has a nice analytic expression:

$$K(\eta) = \frac{(\sinh \eta \cosh \eta - \eta)^{1/3}}{\sinh \eta}, \quad (2.9)$$

and the g^i 's are forms representing the angular directions, given explicitly by

$$g^{1,3} = \frac{e^1 \mp e^3}{\sqrt{2}}, \quad g^{2,4} = \frac{e^2 \mp e^4}{\sqrt{2}}, \quad g^5 = e^5 \quad (2.10)$$

with

$$\begin{aligned} e^1 &= -\sin \theta_1 d\varphi_1, & e^2 &= d\theta_1, & e^3 &= \cos \psi \sin \theta_2 d\varphi_2 - \sin \psi d\theta_2, \\ e^4 &= \sin \psi \sin \theta_2 d\varphi_2 + \cos \psi d\theta_2, & e^5 &= d\psi + \cos \theta_1 d\varphi_1 + \cos \theta_2 d\varphi_2. \end{aligned} \quad (2.11)$$

(For details on the warped deformed conifold, and coordinate systems, see e.g. [18].)

It is also useful to visualise this metric in terms of a proper radial coordinate

$$r(\eta) = \frac{\epsilon^{2/3}}{\sqrt{6}} \int_0^\eta \frac{dx}{K(x)} \quad (2.12)$$

which measures the actual distance up the throat in the six-dimensional metric \tilde{g} . The metric can now be written as:

$$d\tilde{s}_6^2 = dr^2 + r^2 \left[\frac{C_3^2(r)}{9}(g^5)^2 + \frac{C_1^2(r)}{6}\{(g^3)^2 + (g^4)^2\} + \frac{C_2^2(r)}{6}\{(g^1)^2 + (g^2)^2\} \right] \quad (2.13)$$

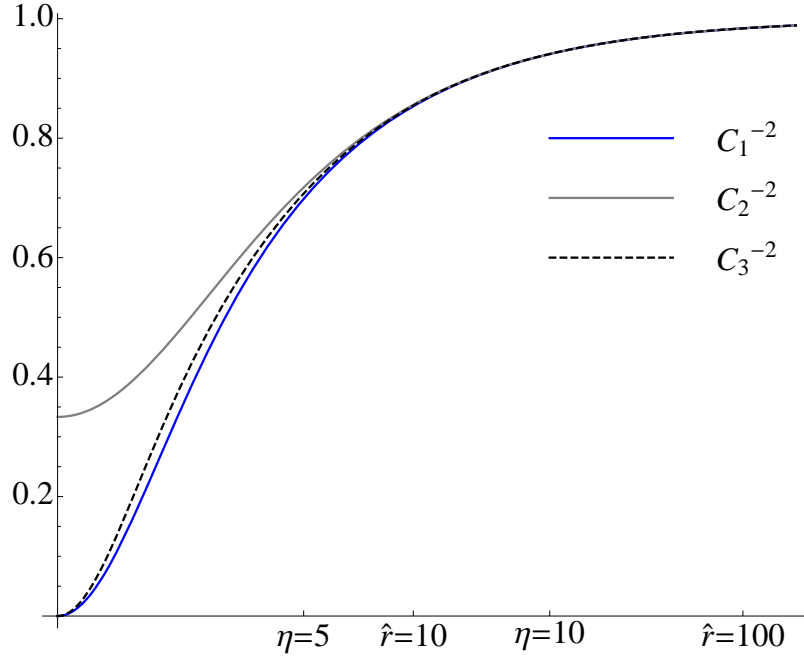


Figure 1: A plot of the metric functions C_i , which shows how the deformation of the conifold increases as the tip is approached. The metric asymptotes the $T^{1,1}$ cone, but near the origin, rC_1 and rC_3 remain finite leaving the nonsingular S^3 metric at the tip of the ‘cone’. The axis is labelled both in terms of the original η coordinate, as well as the normalized proper distance up the throat, $\hat{r} = \epsilon^{-2/3}r$.

where the functions $C_i(r)$ are given implicitly from (2.8), and are shown in figure 1. At small r :

$$r \sim \frac{\epsilon^{2/3}}{3^{1/6}2^{5/6}} \eta \quad , \quad K \simeq \left(\frac{2}{3}\right)^{1/3} \quad (2.14)$$

and the metric (2.13) smoothly closes off at $r = 0$ with a finite S^3 of radius $\epsilon^{2/3}/12^{1/6}$. At large r , or for $\eta \sim 10 - 15$, the C_i ’s become unity, and the throat explicitly takes the form of a cone: $\mathbb{R} \times T^{1,1}$.

In terms of the η coordinate, the warp factor has the form, [17]

$$e^{-4A} = 2(g_s M \alpha')^2 \epsilon^{-8/3} I(\eta), \quad (2.15)$$

where¹

$$I(\eta) \equiv \int_{\eta}^{\infty} dx \frac{x \coth x - 1}{\sinh^2 x} (\sinh x \cosh x - x)^{1/3}. \quad (2.16)$$

Thus for small η

$$\begin{aligned} e^{-4A} &\sim 2(g_s M \alpha')^2 \epsilon^{-8/3} \left[I(0) - \frac{\eta^2}{12} \left(\frac{2}{3}\right)^{1/3} \right] \\ &= 2(g_s M \alpha')^2 \epsilon^{-8/3} \left[0.5699 - \epsilon^{-4/3} \frac{r^2}{3} \right] \end{aligned} \quad (2.17)$$

¹Note that this definition of I relocates a factor of $2^{1/3}$ relative to the KS expression.

and for large η :

$$\begin{aligned} e^{-4A} &\sim 3 \cdot 2^{1/3} (g_s M \alpha')^2 \epsilon^{-8/3} (\eta - 1/4) e^{-4\eta/3} \\ &= \frac{27}{8} \frac{(g_s M \alpha')^2}{r^4} \left(\ln \frac{r^3}{\epsilon^2} + \ln \frac{4\sqrt{2}}{3\sqrt{3}} - \frac{1}{4} \right) \end{aligned} \quad (2.18)$$

which shows how the warp factor interpolates between the Klebanov-Tseytlin (KT) form, [19], for large r , to a smooth cap for $r\epsilon^{-2/3} \lesssim 1$. In addition, for sufficiently small ϵ , there is an intermediate adS region for $|\ln r| \ll |\ln \epsilon^{2/3}|$, in which the logarithmic dependence on r is subdominant to the deformation term.

In an ISD compactification such as the warped deformed conifold, only the complex-structure moduli are stabilized but not the Kähler moduli (that characterize the size of the internal Calabi-Yau). When the no-scale structure is broken to stabilize the Kähler moduli, perturbations around the ISD solution are expected. The Einstein equations and five-form Bianchi identity imply that the perturbations of Φ_- around ISD conditions satisfy, at linear level, the 6D Laplace equation with respect to the unperturbed metric [5, 10]:

$$\tilde{\Delta} \Phi_- = 0. \quad (2.19)$$

This then feeds in to a potential for the D3-brane motion. (See [5] for a detailed explanation and computation of potentials away from the tip of the throat.)

In most inflationary models, the potential is computed away from the tip of the throat, and the geometry is approximated by $AdS_5 \times T^{1,1}$. In this case, the angular part of the Laplace equation, (2.19) is relatively straightforward, and solutions take a particularly clean form:

$$\Phi_-(r, \Psi) = \sum_{L, M} \Phi_{LM} \left(\frac{r}{r_{UV}} \right)^{\Delta(L)} Y_{LM}(\Psi), \quad (2.20)$$

where r is the proper radial distance in the metric \tilde{g}_{mn} , (2.12), and

$$\Delta(L) \equiv -2 + \sqrt{6[l_1(l_1 + 1) + l_2(l_2 + 1) - R^2/8] + 4} \quad (2.21)$$

is the radial eigenfunction weight, coming from the eigenvalues of the angular eigenfunctions, $Y_{LM}(\Psi)$, of the Laplacian on $T^{1,1}$, [20]. $L \equiv (l_1, l_2, R)$, $M \equiv (m_1, m_2)$ label the $SU(2) \times SU(2) \times U(1)_R$ quantum numbers under the corresponding isometries of $T^{1,1}$, and Φ_{LM} are constant coefficients. The leading order terms of interest have the lowest $\Delta(L)$, the smallest eigenvalues corresponding to non-trivial perturbations being

$$\Delta = \frac{3}{2} \quad \text{for } (l_1, l_2, R) = \left(\frac{1}{2}, \frac{1}{2}, 1\right), \quad Y_{LM} \sim \cos \frac{\theta_1}{2} \cos \frac{\theta_2}{2} e^{i(\phi_1 + \phi_2 + \psi)/2} \quad (2.22)$$

$$\Delta = 2 \quad \text{for } (l_1, l_2, R) = (1, 0, 0), (0, 1, 0) \quad Y_{LM} \sim \cos \theta_i. \quad (2.23)$$

In [5], the first mode, (2.22), was used to construct an inflection potential for the inflationary universe, however, this mode is not allowed in the warped deformed conifold, as the $U(1)_R$ isometry is broken to a discrete \mathbb{Z}_2 and therefore (2.22) is forbidden.

The Laplacian on a general warped deformed conifold was computed in [21, 22], although the radial eigenfunctions were not computed explicitly. Fortunately, since we are only interested in the low lying states dependent on only one angle, θ_i , the Laplacian reduces to²

$$\left[\frac{6}{\sinh^2 \eta} \frac{\partial}{\partial \eta} K^2(\eta) \sinh^2 \eta \frac{\partial}{\partial \eta} + \frac{2}{K(\eta)} \frac{\cosh \eta}{\sin \theta_i} \frac{\partial}{\partial \theta_i} \sin \theta_i \frac{\partial}{\partial \theta_i} \right] \Phi_- = 0 \quad (2.24)$$

which for $\ell = 1$ can be solved analytically to obtain the eigenfunction:

$$\Phi_-(\eta, \Psi) \propto (\cosh \eta \sinh \eta - \eta)^{1/3} \cos \vartheta \quad (2.25)$$

where ϑ stands for *either* θ_1 or θ_2 . Since $r \propto e^{\eta/3}$ for large η , it is easy to see that this corresponds to the second eigenfunction, (2.23), of the mid-throat region. Note however that there is no clean expression of this eigenfunction in terms of the radial coordinate

We will thus use this leading order correction to the background near the tip of the throat to investigate the effect of angular perturbations on the brane motion in inflation.

3. Brane inflation with an angular potential

The premise of brane inflation is that a D3-brane, extended in the non-compact dimensions, can move around on the internal manifold in such a way that the ‘scalar’ field y^m , representing the location of the brane on the internal manifold, plays the role of the inflaton. For a mobile D3-brane moving on a supergravity background, the effective action is given by combining the DBI effective action for the worldbrane coordinates, and the Wess-Zumino coupling to the RR-background. Choosing a gauge which aligns with the coordinate system ($X_{D3}^a = (x^\mu, y^m(x^\mu))$), gives the explicit form:

$$\begin{aligned} S_{DBI} + S_{WZ} &= -T_3 \int d^4 \xi \sqrt{-\det(\gamma_{ab} + \mathcal{F}_{ab})} + T_3 \int_{\mathcal{W}} C_4, \\ &= -T_3 \int d^4 x \sqrt{-g} \left[e^{4A} \sqrt{\det(\delta_\nu^\mu - e^{-4A} y^{m,\mu} y_{,\nu}^n \tilde{g}_{mn})} - \alpha \right] \end{aligned} \quad (3.1)$$

where $T_3 = 1/(2\pi)^3 g_s \alpha'^2$ is the D3-brane tension. The energy momentum from this action,

$$T_{\mu\nu} = T_3 \left\{ e^{4A} \sqrt{\det(\delta_\nu^\mu - e^{-4A} y^{m,\mu} y_{,\nu}^n \tilde{g}_{mn})} (g_{\mu\nu} - e^{-4A} y_{,\mu}^m y_{,\nu}^n \tilde{g}_{mn}) - \alpha g_{\mu\nu} \right\} \quad (3.2)$$

²We agree with the correction noted by Pufu et al., [22], to the Laplacian in [21].

can then drive gravitational physics in the noncompact dimensions. In general, there will also be additional terms coming from corrections to the supergravity background which will appear as effective potential terms for the internal coordinates.

The 4D effective gravitational action can be obtained by integrating out (2.1) for the background (2.4):

$$S = -\frac{1}{2\kappa_{10}^2} \int d^{10}x \sqrt{g_{10}} \mathcal{R} \rightarrow -\frac{1}{2\kappa_{10}^2} \left(\int d^6y e^{-4A} \sqrt{\tilde{g}} \right) \int d^4x \sqrt{g} R(g) , \quad (3.3)$$

which gives the 4D Planck mass as

$$M_p^2 = \frac{1}{\kappa_{10}^2} \int e^{-4A} \sqrt{\tilde{g}} d^6y \geq \frac{1}{6g_s^2 \alpha'^4} \left(\frac{\epsilon}{2\pi} \right)^4 \int_0^{\eta_{UV}} e^{-4A} \sinh^2 \eta d\eta , \quad (3.4)$$

and provides a constraint on the parameters of the solution, [23].

For an inflationary solution, we will take the position of the D3 brane to be homogeneous, i.e. $y^m = y^m(t)$, and we will assume an FRW 4D metric:

$$g_{\mu\nu} dx^\mu dx^\nu = dt^2 - a^2(t) d\mathbf{x}^2 . \quad (3.5)$$

Defining the relativistic γ -factor as

$$\gamma = 1 / \sqrt{1 - e^{-4A} \dot{y}^m \dot{y}^n \tilde{g}_{mn}} , \quad (3.6)$$

we can read off the energy and pressure produced by the brane from (3.2) as

$$E = T_3 (e^{4A} [\gamma - 1] + V) \quad (3.7)$$

$$P = T_3 (e^{4A} [1 - \gamma^{-1}] - V) \quad (3.8)$$

where we have rolled any nonzero ($e^{4A} - \alpha$) perturbation, as well as other corrections to the D3-brane potential into V . One correction we will be interested in is a mass term for the canonically normalised radial scalar inflaton, given to leading order by

$$\phi = \sqrt{T_3} r(\eta) \quad (3.9)$$

Note that the normalisation is strictly dependent on the position of the brane, which affects the volume modulus (see e.g. [5]), and also on the trajectory of the brane, even in the slow roll approximation, due to the inflaton, $\phi \leftrightarrow y^m$, being a sigma model field, [24].

The full equations of motion (in terms of the coordinates) are:

$$H^2 = \frac{E}{3M_p^2} \quad (3.10)$$

$$\dot{H} = -\frac{(E + P)}{2M_p^2} \quad (3.11)$$

$$\frac{1}{a^3} \frac{d}{dt} [a^3 \gamma \tilde{g}_{mn} \dot{y}^n] = -2\gamma (\gamma^{-1} - 1)^2 e^{4A} \partial_m A + \frac{\gamma}{2} \frac{\partial \tilde{g}_{ln}}{\partial y^m} \dot{y}^l \dot{y}^n - \partial_m V . \quad (3.12)$$

The first step is to disentangle the radial and angular equations from (3.12), by a process of cross elimination. For simplicity, we will consider motion in a single angular direction only, writing the relevant part of the internal metric in the general form

$$ds^2 = \epsilon^{4/3} \left[\frac{d\eta^2}{6K(\eta)^2} + B(\eta)d\vartheta^2 \right] \quad (3.13)$$

this gives the η and ϑ equations as:

$$\begin{aligned} \ddot{\eta} = & -\frac{3H}{\gamma^2}\dot{\eta} - 4A'(\gamma^{-1} - 1)\dot{\eta}^2 - 12\epsilon^{-4/3}K^2A'e^{4A}(\gamma^{-1} - 1)^2 \\ & + \frac{K'}{K}\dot{\eta}^2 + 3K^2B'\dot{\vartheta}^2 + e^{-4A}\dot{\vartheta}\dot{\eta}\frac{V_{\vartheta}}{\gamma} - (6K^2\epsilon^{-4/3} - e^{-4A}\dot{\eta}^2)\frac{V_{\eta}}{\gamma} \end{aligned} \quad (3.14)$$

$$\ddot{\vartheta} = -\frac{3H}{\gamma^2}\dot{\vartheta} - 4A'(\gamma^{-1} - 1)\dot{\eta}\dot{\vartheta} - \frac{B'}{B}\dot{\eta}\dot{\vartheta} + e^{-4A}\dot{\eta}\dot{\vartheta}\frac{V_{\eta}}{\gamma} - \left(\frac{\epsilon^{-4/3}}{B} - e^{-4A}\dot{\vartheta}^2\right)\frac{V_{\vartheta}}{\gamma} \quad (3.15)$$

These can then be solved numerically, along with the cosmological evolution, for the relevant potential. Generally, potentials can have complicated angular dependence, but we confine ourselves here to the most simple case including only the lowest non-trivial eigenmode with one angular direction. This should be sufficient for estimating the inflationary implications of brane angular dependence.

4. Inflationary analysis

In order to explore the effect of angular terms in the potential, we will use the linearized harmonic function we have computed, (2.25), together with a generic mass term for the inflaton:

$$T_3V = T_3\Phi_- + \frac{1}{2}m_0^2\phi^2 = T_3 \left(\frac{1}{2}m_0^2 [r(\eta)^2 + c_2K(\eta) \sinh \eta \cos \vartheta] + V_0 \right) \quad (4.1)$$

where the constant V_0 is chosen so that the global minimum of V is $V = 0$. Because we are neither slow-rolling, nor restricting ourselves to a specific conical region, we have to keep the full richness of the structure of the internal space and the nonlinear kinetic terms of the brane motion. Although the canonical inflaton field, ϕ , is conventionally used in expositions of slow roll inflation, it proves more useful here to remain with the coordinate label, η , as many of the metric functions have analytic forms in terms of η . We focus on motion which takes place in the angular direction, ϑ , appearing in this potential, thus from (2.8), (2.10) and (2.11) we can read off the function $B = \frac{1}{2}K \cosh \eta$, that appears in the ϑ equation of motion, (3.15).

Before presenting the results of the numerical analysis, a few remarks about the various parameters are in order. First of all, the supergravity approximation is only valid if the curvature remains large compared to the string scale, which clearly requires the flux $g_s M \gg 1$. Secondly, as noted by Baumann and McAllister, [23],

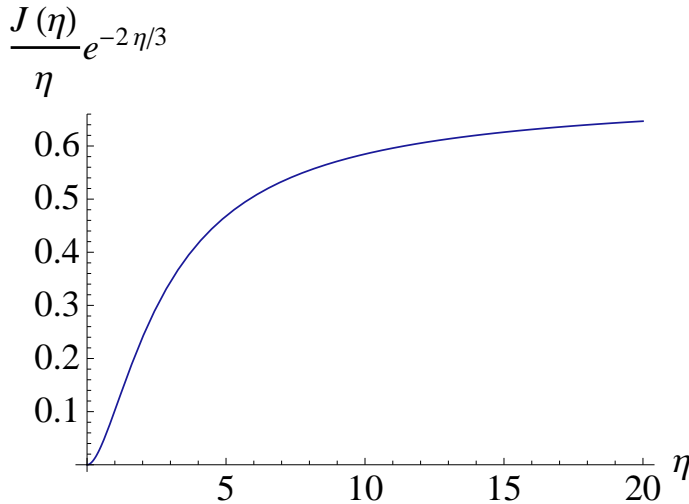


Figure 2: Planck mass constraint: The numerical integral of $I(\eta) \sinh^2 \eta$ with the large η behaviour factored out.

the Planck mass is constrained by the volume of the compactification, which in turn is bounded from the UV cut-off of the throat. Rewriting (3.4) shows that

$$M_p^2 > \frac{\epsilon^{4/3} g_s M^2 T_3}{12\pi} J(\eta_{UV}) \quad (4.2)$$

where $J(\eta)$ is the integral in (3.4), which is exponentially growing in η - see figure 2. This shows clearly that the hierarchy between the string scale and the Planck scale is strongly dependent on the UV cutoff (which determines $J(\eta_{UV})$) and the deformation parameter ϵ . We have already seen that $g_s M^2$ is large, and J_{UV} grows very quickly with η_{UV} , on the other hand, ϵ is generally very small. Recall that the proper distance up the throat, (2.12) scales as $\epsilon^{2/3}$ (as well as depending exponentially on η), thus a small ϵ corresponds to a (logarithmically) larger η_{UV} , and allows for the intermediate $\text{adS} \times T^{1,1}$ regime already discussed. Generally, as the Planck mass rises, the effective scale of inflation is lowered, and thus the amount of inflation can drop unless the parameter choices allow it to persist for a correspondingly increased time (see the discussion after (4.8)). In these models, as in slow-roll inflation, [23], this bound on the Planck mass proves to be a strong constraint.

To solve the full cosmological and brane equations, a numerical analysis is required. For our integrations, we chose $\eta_{UV} = 10$, so that the metric functions are showing evidence of both the throat tip deformation, as well as the asymptotic $T^{1,1}$ structure commonly used in the slow-roll models. The initial radial brane velocity was taken to vanish, and the angular brane velocity either to vanish or to be highly relativistic. The initial value of the angular coordinate, $\vartheta_0 = \pi/2$ was chosen to maximize the impact of the angular term, when present. For the compactification data, we set the Planck mass at its minimum allowed value, as determined by (4.2),

and varied ϵ , M and m_0 , following the motion of the mobile brane with and without the angular term in the potential.

Our findings were the following: In terms of the trajectory of the mobile brane, one feature that all the brane trajectories share is that, independent of any angular dependence or initial momentum, the brane rapidly becomes highly relativistic, and makes its initial sweep in a mostly radial direction, only picking up the detail of angular features near the tip of the throat as inflation per se ends. Figure 3 shows some sample trajectories for the brane as it nears the tip of the throat. Note how the brane approaches from a mostly radial direction before the impact of the angular term makes itself felt at $\eta \simeq 2$. Even in strongly deformed throats, which have a great deal of angular motion near the tip, this initial sweep is strongly radial.

For each trajectory, we followed the brane motion until it settled into oscillations around the minimum of the potential, counting the number of e-foldings of the associated cosmology, to see how this varied with the model parameters. Varying the compactification flux, M , had the effect of slowing the brane motion for increasing M , however, the number of e-foldings and trajectories remain essentially identical. On the other hand, the impact of changing ϵ or m_0 is far more significant.

As the deformation parameter is increased, the brane motion samples more of the angular features of the throat, particularly right near the tip. The brane motion becomes less relativistic, however the amount of expansion dramatically drops and the set-up ceases to be a viable inflationary scenario. Similarly, as the mass of the scalar is decreased, the amount of inflation drops. Decreasing ϵ , or increasing m_0 , slows the coordinate motion of the brane, but increases the number of e-foldings markedly.

Increasing the significance of the angular perturbation (c_2) has the effect of shifting the minimum of the potential, but the effect on the inflationary capacity of the trajectory was sub-dominant. This is indicated in the middle pair of plots of figure 3 where increasing $c_2\epsilon^{-4/3}$ from 0.5 to 0.9 increases the expansion by about 5%. In more detail, figure 4 shows a plot of the number of e-foldings as a function of time along an inflationary trajectory with $m_0 = 5$, $g_s M = 100$, $\epsilon = 0.001$ and compares the amount of inflation with and without angular dependence in the potential. This clearly shows the subdominance of angular terms, illustrating that the bulk of inflation occurs along the initial, radial, sweep.

One way to see how these dependencies arise is to rescale the equations of motion by setting $\tau = \epsilon^{2/3}t/(g_s M \alpha')$, and rewriting the metric functions as:

$$\hat{h} = \frac{\epsilon^{8/3}}{(g_s M \alpha')^2} e^{-4A} \quad , \quad \hat{V} = \epsilon^{-4/3} V \quad (4.3)$$

so that \hat{h} and \hat{V} now have no ϵ or M dependence. Note also that

$$\gamma^{-2} = 1 - \hat{h} \left[\frac{\dot{\eta}^2}{6K^2} + B\dot{\vartheta}^2 \right] \quad (4.4)$$

where a dot now denotes $d/d\tau$, also has no ϵ or M dependence.

Setting $\alpha' = 1$, the full equations of motion of the system now read:

$$\hat{H}^2 = \frac{T_3}{3M_p^2} \left[(g_s M)^2 \hat{V} + \frac{\epsilon^{4/3}}{\hat{h}} (\gamma - 1) \right] \longrightarrow 4\pi g_s \left[\epsilon^{-4/3} \hat{V} + \frac{\gamma - 1}{(g_s M)^2 \hat{h}} \right] \quad (4.5)$$

$$\dot{\hat{H}} = -\frac{\epsilon^{4/3} T_3}{6M_p^2 \hat{h}} (\gamma - \gamma^{-1}) \longrightarrow -\frac{2\pi(\gamma - \gamma^{-1})}{g_s M^2 \hat{h}} \quad (4.6)$$

$$\begin{aligned} \ddot{\eta} = & -\frac{3\hat{H}}{\gamma^2} \dot{\eta} + \frac{\hat{h}'}{\hat{h}} (\gamma^{-1} - 1) \dot{\eta}^2 + 3K^2 \frac{\hat{h}'}{\hat{h}^2} (\gamma^{-1} - 1)^2 \\ & + \frac{K'}{K} \dot{\eta}^2 + 3K^2 B' \dot{\vartheta}^2 + \frac{(g_s M)^2}{\epsilon^{4/3} \gamma} \left[\hat{h} \dot{\eta} \dot{\eta} \hat{V}_{\vartheta} - (6K^2 - \hat{h} \dot{\eta}^2) \hat{V}_{\eta} \right] \end{aligned} \quad (4.7)$$

$$\ddot{\vartheta} = -\frac{3\hat{H}}{\gamma^2} \dot{\vartheta} + \left[\frac{\hat{h}'}{\hat{h}} (\gamma^{-1} - 1) - \frac{B'}{B} \right] \dot{\eta} \dot{\vartheta} + \frac{(g_s M)^2}{\epsilon^{4/3} \gamma} \left[\hat{h} \dot{\eta} \dot{\vartheta} \hat{V}_{\eta} - (1 - \hat{h} B \dot{\vartheta}^2) \frac{\hat{V}_{\vartheta}}{B} \right] \quad (4.8)$$

where we have shown the effect of saturating the Planck mass bound. We can now see not only that the effect of the flux and deformation parameter is to increase the importance of the potential in the brane motion, but also that with the Planck mass bound saturated, the Hubble parameter is strongly dependent on ϵ , but the impact of the flux is sub-dominant. Crudely therefore, we can see how increasing m_0 or decreasing ϵ has a strong effect on the number of e-foldings, and the time rescaling shows how these parameters impact on the coordinate velocities.

Finally, although these equations must be solved numerically to extract the actual cosmological impact, an estimate for the number of e-foldings can be approximated analytically. From the numerics, the bulk of cosmological expansion occurs on the first sweep down the throat of the brane, and this motion is roughly radial. Approximating this motion as precisely radial, the number of e-foldings of the universe, \mathcal{N} , can be written as

$$\mathcal{N} = \int H dt = \int \frac{H}{\dot{\eta}} d\eta \quad (4.9)$$

and we can approximate

$$H^2 \sim \frac{T_3 V}{3M_p^2} \quad , \quad \frac{\epsilon^{4/3} e^{-4A} \dot{\eta}^2}{6K^2} \sim 1 \quad (4.10)$$

giving

$$\mathcal{N} \sim \sqrt{\frac{T_3}{3M_p^2}} \int \sqrt{\frac{V}{6}} e^{-2A} \frac{d\eta}{K} \leq \frac{\epsilon^{-2/3} m_0 \sqrt{4\pi g_s}}{6J_{UV}} \int_{\eta_f}^{\eta_i} \frac{I(\eta) \epsilon^{-2/3} r(\eta)}{6K} d\eta \quad (4.11)$$

The ratio of the integral to J_{UV} is explicitly independent of the various parameters, and only depends on η_{UV} .

This argument is somewhat flawed in that it uses a large γ factor to estimate the coordinate velocity, yet assumes that the γ terms are negligible compared to

the potential, nonetheless, it gives a good guide as to the general dependence of the e-foldings from brane motion near the tip, which is reasonably accurate for small ϵ as can be seen by comparing the numerical and analytical results in figure 5. In this plot we see clearly that for $\epsilon \leq 0.01$, the estimate gives a very good approximation to the dependence of \mathcal{N} on ϵ . For strongly deformed throats ($\epsilon \geq 0.1$) the estimate does not work so well, but since these have much more varied angular motion and very few e-foldings, this is not at all surprising. Unlike the small ϵ trajectories, which spend a very long time on the initial radial sweep, exiting inflation very close to the minimum of the potential, these trajectories fall reasonably quickly to the tip, and cosmological expansion takes place equally from the initial sweep as from the following large angular oscillations.

5. Summary and conclusions

In this paper we studied generic brane motion in a warped deformed throat incorporating full angular dependence of both the brane potential and brane motion. We considered a generic mass term for the D3 brane potential as well as an analytic linearized perturbation around the ISD background, which to our knowledge is the first closed form analytic radial eigenfunction on the KS background.

Our results show that angular features of the brane motion are dependent on the compactification parameters more than on initial conditions: For strongly deformed throats (relatively large ϵ) the brane ‘sees’ the full rounded structure of the tip and has a very rich angular motion. These oscillatory trajectories however have very little cosmological expansion. Conversely, for very sharp throats ($\epsilon \ll 1$) the brane enters a strongly DBI inflating motion, which is geometry dominated and mainly radial in nature. The coordinate velocities of the brane are very small, and the brane falls to the minimum of the potential in its first sweep down the throat, only oscillating right at the exit of inflation and at the minimum of the potential.

In all cases, the DBI trajectories have large γ factors and hence will most likely generate large non-gaussianities, [9, 25], rendering these models unsatisfactory as inflation models in their own right. However, as the γ factor varies throughout the motion, it is possible that for some carefully chosen parameters this problem could be circumvented. However, it is interesting to use the intuition gleaned here to consider the late time evolution of more conventional slow-roll brane models, and explore what might happen as the brane approaches the tip.

A slow-roll model such as the delicate universe, [5], has perturbations which are strictly only allowed in the pure $T^{1,1}$ throat, however, setting this aside for a moment, we can speculate on the final brane downfall to the tip. A vast scanning of parameter space for potentials is not necessary, as the angular motion and dependence is more a quantitative than qualitative factor, and our investigation has given insight into the effect of the different compactification parameters as they vary.

Typically, a slow roll model of brane inflation will be in the intermediate adS regime of the throat geometry, and thus requires a small deformation parameter. However, as the deformation parameter becomes very small, the final roll to the tip can take a long time, and be highly relativistic. The compactification data are generally expressed differently in references [5, 11], in terms of D3 flux, N , the warp hierarchy between the inflating and IR region, $a_0 = e^{A(0)}$, however, knowledge of M_p , T_3 and the UV cut-off scale of the throat, r_{UV} , allows a translation between the different parametrizations. For example, to compare to the study of Agarwal et al., [11], saturating the M_p bound and taking their stated parameter values leads to deformation parameters of $\epsilon \sim 10^{-4} - 10^{-7}$ for $a_0 \sim 10^{-3} - 10^{-5}$. With such small deformation parameters, the final sweep to the throat tip could easily incorporate several to many e-foldings of DBI inflation, and raises the question of just how much impact this final sweep could have.

Finally, our analysis has focussed on motion in only one angular direction. This was primarily to allow clarity of the angular terms in the potential, but also for simplicity. We expect that including fully generic angular motion (which would significantly complicate the analysis) will have an effect subdominant to the subdominant angular motion presented here, however, it would be useful to confirm this. In addition, our analysis could be further extended by taking higher order corrections into account, which will also have angular dependence. While we would expect that this would be sub-dominant to the linearized correction, it would be interesting to see precisely what the impact is of these detailed corrections to the inflaton potential.

Acknowledgments

We would like to thank Gianmassimo Tasinato for helpful comments. This work was supported in part by STFC under the rolling grant ST/G000433/1. RG would like to acknowledge the Aspen Center for Physics, NSF grant 1066293, for hospitality while this work was finished.

References

- [1] S. Kachru, R. Kallosh, A. D. Linde and S. P. Trivedi, Phys. Rev. D **68**, 046005 (2003) [arXiv:hep-th/0301240].
- [2] G. R. Dvali and S. H. H. Tye, Phys. Lett. B **450**, 72 (1999) [arXiv:hep-ph/9812483].
S. H. S. Alexander, Phys. Rev. D **65**, 023507 (2002) [arXiv:hep-th/0105032].
C. P. Burgess, M. Majumdar, D. Nolte, F. Quevedo, G. Rajesh and R. J. Zhang, JHEP **0107**, 047 (2001) [arXiv:hep-th/0105204].
G. Shiu and S. H. H. Tye, Phys. Lett. B **516**, 421 (2001) [arXiv:hep-th/0106274];
- [3] S. Kachru, R. Kallosh, A. D. Linde, J. M. Maldacena, L. P. McAllister and S. P. Trivedi, JCAP **0310**, 013 (2003) [arXiv:hep-th/0308055].

- [4] H. Firouzjahi and S. H. H. Tye, Phys. Lett. B **584**, 147 (2004) [arXiv:hep-th/0312020].
 C. P. Burgess, J. M. Cline, K. Dasgupta and H. Firouzjahi, JHEP **0703**, 027 (2007) [arXiv:hep-th/0610320].
 F. Chen and H. Firouzjahi, JHEP **0811**, 017 (2008) [arXiv:0807.2817 [hep-th]].
 H. Y. Chen, J. O. Gong and G. Shiu, JHEP **0809**, 011 (2008) [arXiv:0807.1927 [hep-th]].
 H. Y. Chen and J. O. Gong, Phys. Rev. D **80**, 063507 (2009) [arXiv:0812.4649 [hep-th]].
- [5] D. Baumann, A. Dymarsky, I. R. Klebanov, J. M. Maldacena, L. P. McAllister and A. Murugan, JHEP **0611**, 031 (2006) [arXiv:hep-th/0607050].
 D. Baumann, A. Dymarsky, I. R. Klebanov, L. McAllister and P. J. Steinhardt, Phys. Rev. Lett. **99**, 141601 (2007) [arXiv:0705.3837 [hep-th]].
 D. Baumann, A. Dymarsky, I. R. Klebanov and L. McAllister, JCAP **0801**, 024 (2008) [arXiv:0706.0360 [hep-th]].
 D. Baumann, A. Dymarsky, S. Kachru, I. R. Klebanov and L. McAllister, JHEP **0903**, 093 (2009) [arXiv:0808.2811 [hep-th]].
 D. Baumann, A. Dymarsky, S. Kachru, I. R. Klebanov and L. McAllister, Phys. Rev. Lett. **104**, 251602 (2010) [arXiv:0912.4268 [hep-th]].
 D. Baumann, A. Dymarsky, S. Kachru, I. R. Klebanov and L. McAllister, JHEP **1006**, 072 (2010) [arXiv:1001.5028 [hep-th]].
- [6] S. Kecskemeti, J. Maiden, G. Shiu and B. Underwood, JHEP **0609**, 076 (2006) [arXiv:hep-th/0605189].
 O. DeWolfe, L. McAllister, G. Shiu and B. Underwood, JHEP **0709**, 121 (2007) [arXiv:hep-th/0703088].
 E. Pajer, JCAP **0804**, 031 (2008) [arXiv:0802.2916 [hep-th]].
- [7] H. Y. Chen, J. O. Gong, K. Koyama and G. Tasinato, JCAP **1011**, 034 (2010) [arXiv:1007.2068 [hep-th]].
- [8] S. H. Henry Tye, Lect. Notes Phys. **737**, 949 (2008) [arXiv:hep-th/0610221].
 J. M. Cline, “String cosmology,” arXiv:hep-th/0612129.
 R. Kallosh, Lect. Notes Phys. **738**, 119 (2008) [arXiv:hep-th/0702059].
 C. P. Burgess, Class. Quant. Grav. **24**, S795 (2007) [arXiv:0708.2865 [hep-th]].
 L. McAllister and E. Silverstein, Gen. Rel. Grav. **40**, 565 (2008) [arXiv:0710.2951 [hep-th]].
- [9] E. Silverstein and D. Tong, Phys. Rev. D **70**, 103505 (2004) [arXiv:hep-th/0310221].
 M. Alishahiha, E. Silverstein and D. Tong, Phys. Rev. D **70**, 123505 (2004) [arXiv:hep-th/0404084].
- [10] S. B. Giddings, S. Kachru and J. Polchinski, Phys. Rev. D **66**, 106006 (2002) [arXiv:hep-th/0105097].

- [11] N. Agarwal, R. Bean, L. McAllister and G. Xu, “Universality in D-brane Inflation,” arXiv:1103.2775 [].
- [12] S. Kachru and L. McAllister, JHEP **0303**, 018 (2003) [arXiv:hep-th/0205209].
C. P. Burgess, P. Martineau, F. Quevedo and R. Rabadan, JHEP **0306**, 037 (2003) [arXiv:hep-th/0303170].
C. P. Burgess, F. Quevedo, R. Rabadan, G. Tasinato and I. Zavala, JCAP **0402**, 008 (2004) [arXiv:hep-th/0310122].
- [13] D. A. Easson, R. Gregory, G. Tasinato and I. Zavala, JHEP **0704**, 026 (2007) [arXiv:hep-th/0701252].
- [14] C. Germani, N. E. Grandi and A. Kehagias, Class. Quant. Grav. **25**, 135004 (2008) [arXiv:hep-th/0611246].
- [15] A. Kehagias and E. Kiritsis, JHEP **9911**, 022 (1999) [arXiv:hep-th/9910174].
- [16] D. A. Easson, R. Gregory, D. F. Mota, G. Tasinato and I. Zavala, JCAP **0802**, 010 (2008) [arXiv:0709.2666].
D. A. Easson and R. Gregory, Phys. Rev. D **80**, 083518 (2009) [arXiv:0902.1798].
D. A. Easson, S. Mukohyama and B. A. Powell, Phys. Rev. D **81**, 023512 (2010) [arXiv:0910.1353].
Y. F. Cai, J. B. Dent and D. A. Easson, “Warm DBI Inflation,” arXiv:1011.4074.
- [17] I. R. Klebanov and M. J. Strassler, JHEP **0008**, 052 (2000) [arXiv:hep-th/0007191].
- [18] P. Candelas and X. C. de la Ossa, Nucl. Phys. B **342**, 246 (1990).
R. Minasian and D. Tsimpis, Nucl. Phys. B **572**, 499 (2000) [arXiv:hep-th/9911042].
C. P. Herzog, I. R. Klebanov and P. Ouyang, “Remarks on the warped deformed conifold,” arXiv:hep-th/0108101.
- [19] I. R. Klebanov and A. A. Tseytlin, Nucl. Phys. B **578**, 123 (2000) [arXiv:hep-th/0002159].
- [20] S. S. Gubser, Phys. Rev. D **59**, 025006 (1999) [arXiv:hep-th/9807164].
A. Ceresole, G. Dall’Agata and R. D’Auria, JHEP **9911**, 009 (1999) [arXiv:hep-th/9907216].
- [21] C. Krishnan and S. Kuperstein, JHEP **0805**, 072 (2008) [arXiv:0802.3674].
- [22] S. S. Pufu, I. R. Klebanov, T. Klose and J. Lin, J. Phys. A **44**, 055404 (2011) [arXiv:1009.2763].
- [23] D. Baumann and L. McAllister, Phys. Rev. D **75**, 123508 (2007) [arXiv:hep-th/0610285].
- [24] C. Gordon, D. Wands, B. A. Bassett and R. Maartens, Phys. Rev. D **63**, 023506 (2001) [arXiv:astro-ph/0009131].

- S. Groot Nibbelink and B. J. W. van Tent, *Class. Quant. Grav.* **19**, 613 (2002) [arXiv:hep-ph/0107272].
- A. Achucarro, J. O. Gong, S. Hardeman, G. A. Palma and S. P. Patil, *JCAP* **1101**, 030 (2011) [arXiv:1010.3693 [hep-ph]].
- [25] D. Langlois and S. Renaux-Petel, *JCAP* **0804**, 017 (2008) [arXiv:0801.1085 [hep-th]].
- M. x. Huang, G. Shiu and B. Underwood, *Phys. Rev. D* **77**, 023511 (2008) [arXiv:0709.3299 [hep-th]].
- D. Langlois, S. Renaux-Petel, D. A. Steer and T. Tanaka, *Phys. Rev. Lett.* **101**, 061301 (2008) [arXiv:0804.3139 [hep-th]].
- S. Renaux-Petel and G. Tasinato, *JCAP* **0901**, 012 (2009) [arXiv:0810.2405 [hep-th]].

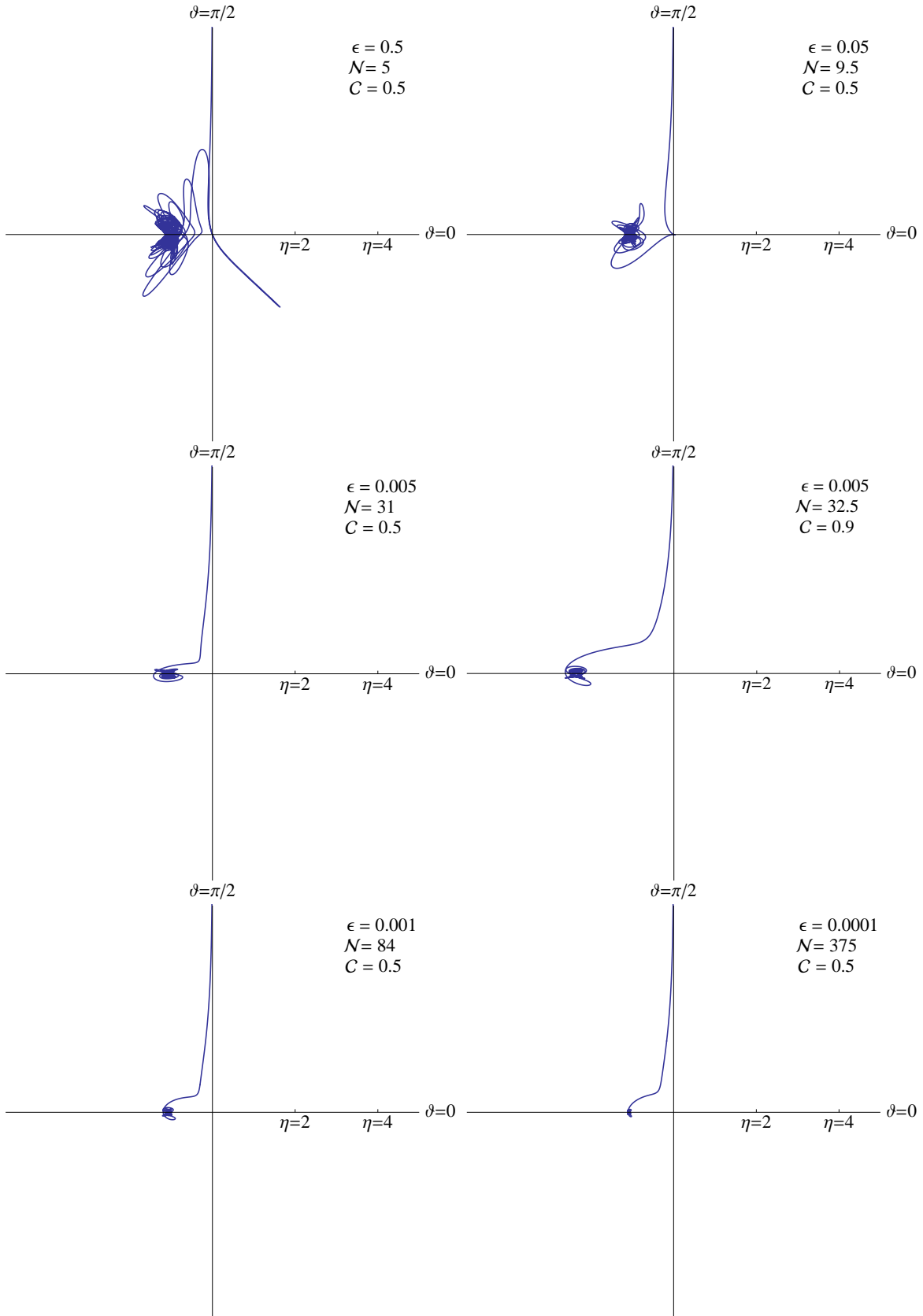


Figure 3: Some sample inflationary trajectories with a flux parameter of $g_s M = 100$, inflaton mass $m_0 = 5$, and a saturated Planck mass. The values of ϵ and $C = c_2 \epsilon^{-4/3}$, are indicated.

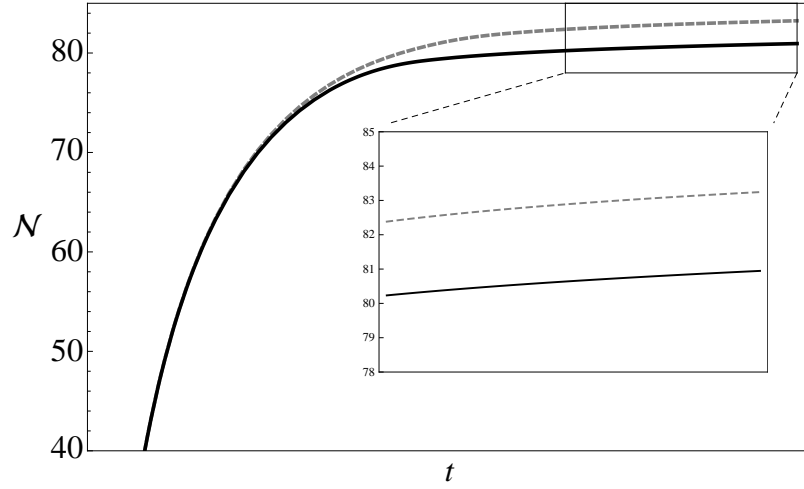


Figure 4: The amount of inflation along a trajectory with $m_0 = 5$, $g_s M = 100$, $\epsilon = 0.001$ with (grey dashed, $c_2 = \epsilon^{4/3}/2$) and without (solid black) angular terms in the potential.

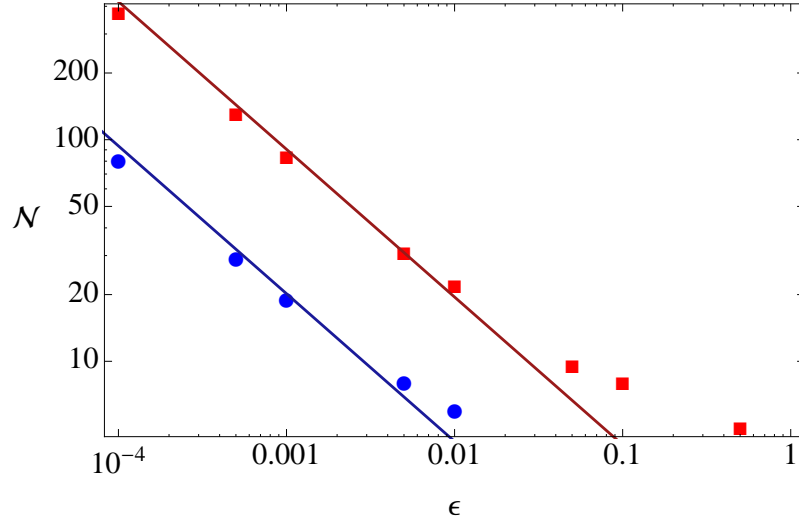


Figure 5: The number of e-foldings as a function of the deformation parameter ϵ for $m_0 = 1$ (blue circles) and $m_0 = 5$ (red squares) with $c_2 = \epsilon^{4/3}/2$ and $g_s M = 100$. The analytic dependence is shown for comparison.